Talanta 118 (2014) 90–95

Contents lists available at ScienceDirect

Talanta

journal homepage: www.elsevier.com/locate/talanta

Rapid visual detection of quaternary ammonium surfactants using citrate-capped silver nanoparticles (Ag NPs) based on hydrophobic effect

Li-Qing Zheng, Xiao-Dong Yu *, Jing-Juan Xu, Hong-Yuan Chen

State Key Laboratory of Analytical Chemistry for Life Science, School of Chemistry and Chemical Engineering, Nanjing University, Nanjing 210093, PR China

ARTICLE INFO

Article history:
Received 23 July 2013
Received in revised form
29 September 2013
Accepted 3 October 2013
Available online 9 October 2013

Keywords:
Colorimetric detection
Citrate-capped silver nanoparticles
Cationic surfactants
Hydrophobic effect

ABSTRACT

In this work, a rapid, sensitive and low-cost colorimetric method for detection of quaternary ammonium surfactants using citrate-capped silver nanoparticles (Ag NPs) was developed. The quaternary ammonium surfactants induce the aggregation of Ag NPs through the hydrophobic effect, which is a novel aggregation mechanism of Ag NPs. The addition of cationic surfactant results in color change of Ag NPs solution from yellow to red and finally to colorless, which is due to the broadening of the surface plasmon band. The color change was monitored using a UV–vis spectrophotometer. The LOD of different cationic surfactants was in the range of 0.5–5 μM. More importantly, this detection method was successfully utilized to the disinfectant residual sample.

Crown Copyright © 2013 Published by Elsevier B.V. All rights reserved.

1. Introduction

The quaternary ammonium surfactants are widely used in industrial applications and pharmaceutical/cosmetic preparations. For example, Myristyltrimethylammonium Bromide (TTAB) is an important component of eye drops and Benzalkonium Bromide (BZKB) is the main component of the disinfectant fluid. However an allergic reaction or inflammation could be induced by them in some sensitive people. What is worse, surfactants become environmental pollutants when they are deposited on land or into water systems [1]. Therefore, the detections of TTAB, BZKB and other quaternary ammonium surfactants are very important. The reported methods include capillary electrophoresis (CE) [2], two-phase titration [3], reversed-phase high-performance liquid chromatographic (RP-HPLC) [4,5], gas chromatography (GC) [6], gas chromatography–mass spectrometry (GC–MS) [7] etc. These methods require large and expensive equipments, complicated operating steps and are time-consuming, and they are quite inconvenient for outdoor detection. So it is necessary to develop simple, rapid and sensitive methods for the detection of quaternary ammonium surfactants.

In recent years, colorimetric detection has attracted much attention because of its low cost, simplicity and practicality [8,9]. Compared to other assays, it allows direct and on-site analysis of the samples with the naked eye [10]. Gold nanoparticles (Au NPs) and silver nanoparticles (Ag NPs) have been widely used to develop high sensitivity colorimetric sensors for biological and chemical detection due to their special optical properties and biocompatibility [11,12]. Varieties of colorimetric sensing based on Au NPs and Ag NPs for different analytes including bacteria [12,13], DNA [14], proteins [15,16], growth factor [17,18], small molecules [19–21] and metal ions [10,22–24] have been developed. For colorimetric assays, Ag NPs have some attractive advantages over Au NPs since they possess higher extinction coefficients relative to Au NPs of the same size and they detect analytes at less material consumption and lower cost than Au NPs [25].

The mechanisms of colorimetric sensing by Au NPs and Ag NPs were based on the aggregation of metal nanoparticles. The aggregation could be induced by electrostatic interaction between negative ion and positive ion [26], complexation with ligand [27–30], the charge transfer interactions between an electron donor and electron acceptor [31], thiolated or disulfide modified ligands [32], antibody–antigen associations [33], and streptavidin–biotin binding [34]. However, to the best of our knowledge, the Ag nanoparticles' aggregation induced by the hydrophobic interaction has not been reported before.

In this paper, a rapid, sensitive and low-cost colorimetric method for detection of cationic surfactants based on the hydrophobic effect is developed. The strategy is illustrated in Scheme 1. Quaternary ammonium surfactants were adsorbed onto the surface of citrate-capped Ag NPs by electrostatic attraction and the surface of Ag NPs became hydrophobic. Then Ag NPs aggregated through the

* Corresponding author. Tel./fax: +86 25 83592774.
E-mail address: yuxd@nju.edu.cn (X.-D. Yu).

0039-9140/$ - see front matter Crown Copyright © 2013 Published by Elsevier B.V. All rights reserved.
http://dx.doi.org/10.1016/j.talanta.2013.10.009

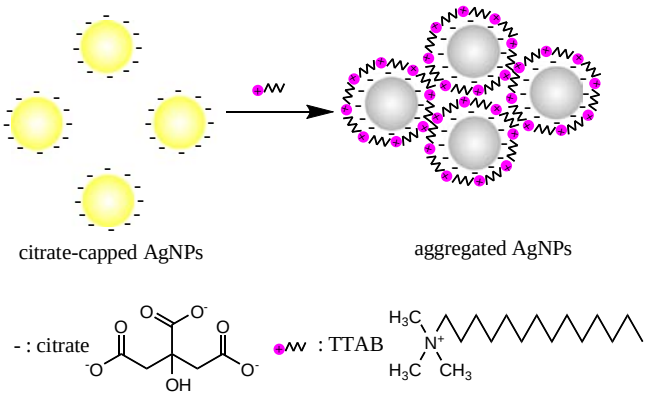

Scheme 1. Schematic mechanism for TTAB inducing the aggregation of citrate-capped Ag NPs.

hydrophobic interaction. The color of Ag NPs solution changed from yellow to red then colorless in the presence of cationic surfactants, which indicated different degrees of the aggregation. This is the first report about the detection of cationic surfactants based on the colorimetric method using Ag NPs. What is more, it has been successfully applied to determine the concentration of BZKB in disinfectant residual sample.

2. Experimental

2.1. Chemicals

Silver nitrate, trisodium citrate, sodium borohydride ($NaBH_4$), sodium chloride (NaCl), sodium sulfate (Na_2SO_4), sodium sulfite (Na_2SO_3), sodium phosphate (Na_3PO_4), sodium nitrate ($NaNO_3$), hydrochloric acid, nitric acid and sulfuric acid were purchased from Nanjing Chemical Reagent Co. Ltd. (Nanjing, China). Sodium perchlorate ($NaClO_4$) was purchased from Tianjin Kemiou Chemical Reagent Co. Ltd. (Tianjin,China). Dodecyl Trimethyl Ammonium Bromide (DTAB), Myristyltrimethylammonium Bromide (TTAB), Cetrimonium Bromide (CTAB), Trimethylstearylammonium Bromide (STAB) and Benzalkonium Bromide (BZKB) were purchased from Sigma-Aldrich (Milwaukee, WI). All the chemicals were analytical-grade reagents and used without further purification. The water used throughout all experiments was purified by an Elix 5 Pure Water System (Millipore, USA).

2.2. Apparatus

UV measurements were performed with a UV-3600 spectrophotometer (Shimadzu, Japan). Transmission electron microscopy (TEM) was recorded by a JEM-2100 electron microscope (JEOL, Japan) operating at 200 kV. The Zeta potential measurements were performed by a Nano-Z system (Malvern Instruments Ltd., UK).

2.3. Preparation of citrate-stabilized Ag NPs.

Ag NPs were prepared using a simple method. 100 mL of 0.1 mM trisodium citrate was added into 100 mL of 0.1 mM $AgNO_3$ under stirring. Then 9 mg $NaBH_4$ was added rapidly into the above aqueous solution under vigorous stirring. This solution was further stirred for 2 h at room temperature. The resulting bright yellow colloidal silver nanoparticles were finally obtained.

2.4. Spectral studies and cationic surfactant detection

In a typical titration, cationic surfactant solution with a given concentration was added to Ag NPs solution containing 10^{-3} M HNO_3 at room temperature. The absorbance spectra and photographs of the solution were recorded 4 min after the addition of analytes.

3. Results and discussion

3.1. Characterization and aggregation of Ag NPs

The citrate-capped Ag NPs were prepared by $NaBH_4$ reduction of $AgNO_3$ with sodium citrate. The TEM images of the dispersed Ag NPs and the aggregated Ag NPs are shown in Fig. 1. From Fig. 1A, it can be seen that the size of Ag NPs is ca. 10 nm. As shown in Fig. 1B, after the addition of 10 μM TTAB, Ag NPs distinctly aggregated.

The citrate-capped Ag NPs turned out to be highly sensitive to TTAB. As shown in Fig. 2A, when 10 μM TTAB was added to the citrate-capped Ag NPs solution, the color of the suspension obviously changed from yellow to nearly colorless within one minute indicating the aggregation of Ag NPs. Detailed study was carried out with UV–vis spectroscopy. As can be seen in Fig. 2B, the characteristic absorption wavelength of Ag NPs at 400 nm was sharply decreased and the absorbance spectrum gradually broadened to a long wave with the addition of 10 μM TTAB.

3.2. Optimization of conditions

3.2.1. Reaction time

To investigate when the aggregation reached equilibrium, the time-dependent UV–vis spectra were recorded. The increase of the

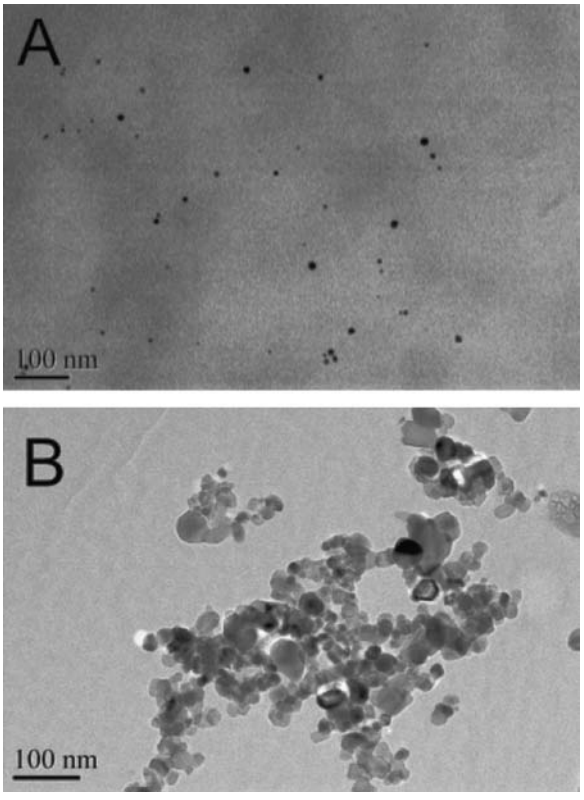

Fig. 1. TEM images of citrate-capped Ag NPs (A) before and (B) after addition of TTAB (10 μM).

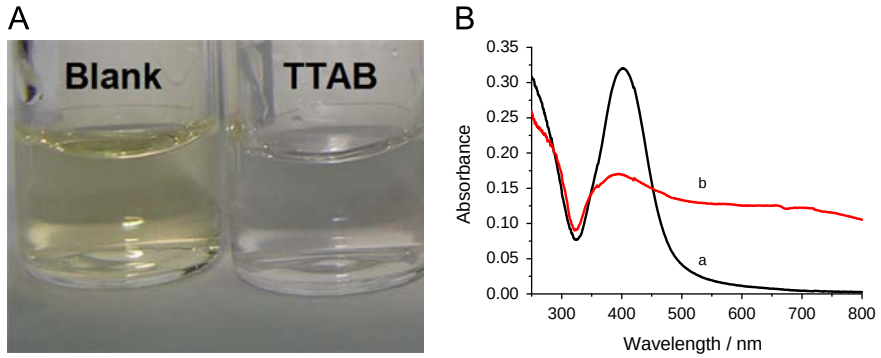

Fig. 2. (A) The color change of the Ag NPs solution with the addition of 10 μM TTAB. (B) The corresponding absorption spectrum of the Ag NPs solution before (a) and after (b) the addition of 10 μM TTAB.

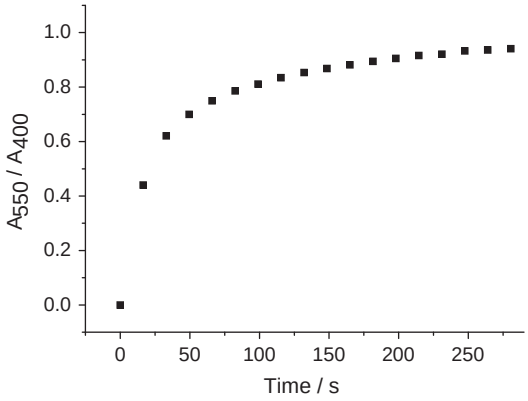

Fig. 3. Time-dependent absorbance changes of the Ag NPs solution with addition of 10 μM TTAB.

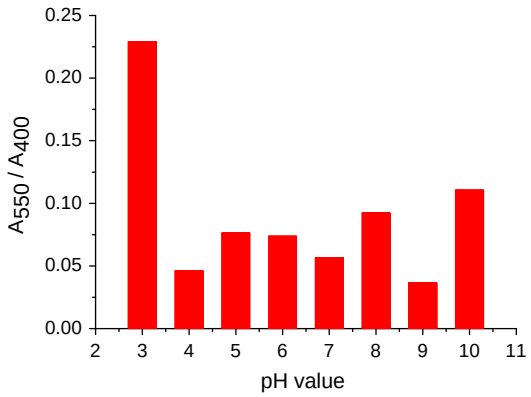

Fig. 4. Absorbance ratio A_{550}/A_{400} of the Ag NPs solutions with addition of 1 μM TTAB against pH.

absorbance ratio A_{550}/A_{400} indicates the aggregation of Ag NPs [35]. In Fig. 3, the absorbance ratio A_{550}/A_{400} increases as the reaction time is prolonged, and it levels off to a saturation value after ca. 4 min. Therefore all the photographing and measurements were carried out after the addition of the analyte for 4 min.

3.2.2. pH

Since the pH values and ionic strength of the solution have effects on the aggregation of Ag NPs, the optimization of the experiment conditions for colorimetric sensing was carried out. The absorbance ratios A_{550}/A_{400} of Ag NPs solutions with addition of 1 μM TTAB under different pH conditions are shown in Fig. 4. It can be seen that the absorbance ratio A_{550}/A_{400} reached the maximum value at pH 3, which indicated the most aggregation of Ag NPs. Thus pH 3 was chosen as the optimal pH for this experiment.

To investigate the influence of different acid on the aggregation of Ag NPs with TTAB, UV–vis spectra of Ag NPs suspension in the presence of 10^{-3} M different acids with addition of TTAB were recorded. As shown in Fig. 5, the characteristic absorption wavelength of Ag NPs at 400 nm was obviously decreased upon the addition of 10^{-3} M H_2SO_4, indicating the aggregation of Ag NPs. In 10^{-3} M HCl or 10^{-3} M HNO_3 solutions Ag NPs could not aggregate and then the absorption of the solution at 400 nm did not change. Compared with HCl and HNO_3, results showed that the absorption of Ag NPs suspension containing 10^{-3} M HCl at 400 nm decreased slightly than the one which contained 10^{-3} M HNO_3 upon the addition of 10^{-6} M TTAB. The decrease of the absorption of the solution at 400 nm is ascribed to the aggregation of Ag NPs induced by TTAB, because of the strong size-dependent SPR properties of nanoparticles [36,37]. The molecular volume of NO_3^- is more than Cl^-, so the hydrophobicity of the ion pair formed by NO_3^- and cationic ammonium surfactant is stronger than that formed by Cl^- and cationic ammonium surfactant. Therefore it is easier for TTAB to induce the aggregation of Ag NPs in the 10^{-3} M HNO_3 solution. So 10^{-3} M HNO_3 was chosen as the optimal experiment condition.

3.2.3. Effect of ionic strength

The influence of $NaClO_4$, NaCl, $NaNO_3$, Na_2SO_3, Na_3PO_4 and Na_2SO_4 on the aggregation of Ag NPs was also studied. The results showed that 10^{-3} M ClO_4^-, Cl^-, NO_3^-, SO_3^{2-} and PO_4^{3-} did not interfere with the detection, while 10^{-4} M SO_4^{2-}, 10^{-2} M Cl^-, ClO_4^-, NO_3^-, SO_3^{2-} and PO_4^{3-} could interfere with the detection (Fig. S1).

3.3. Determination of different cationic surfactants

3.3.1. Myristyltrimethylammonium Bromide (TTAB)

To verify this simple assay for the direct colorimetric visualization of cationic surfactants, the sensitivity was evaluated and the results were displayed in Fig. 6. With the increase in concentration of TTAB in the solution of Ag NPs, the color of the solution changed from yellow to red then finally to nearly colorless. The LOD of TTAB is 3 μM. In addition, as seen in Fig. 6B, with the increasing concentration of TTAB, the characteristic absorbance of Ag NPs at 400 nm gradually decreased; meanwhile, the absorbance spectrum gradually broadened to long wave, which indicated that more and more Ag NPs aggregated. The concentration of TTAB

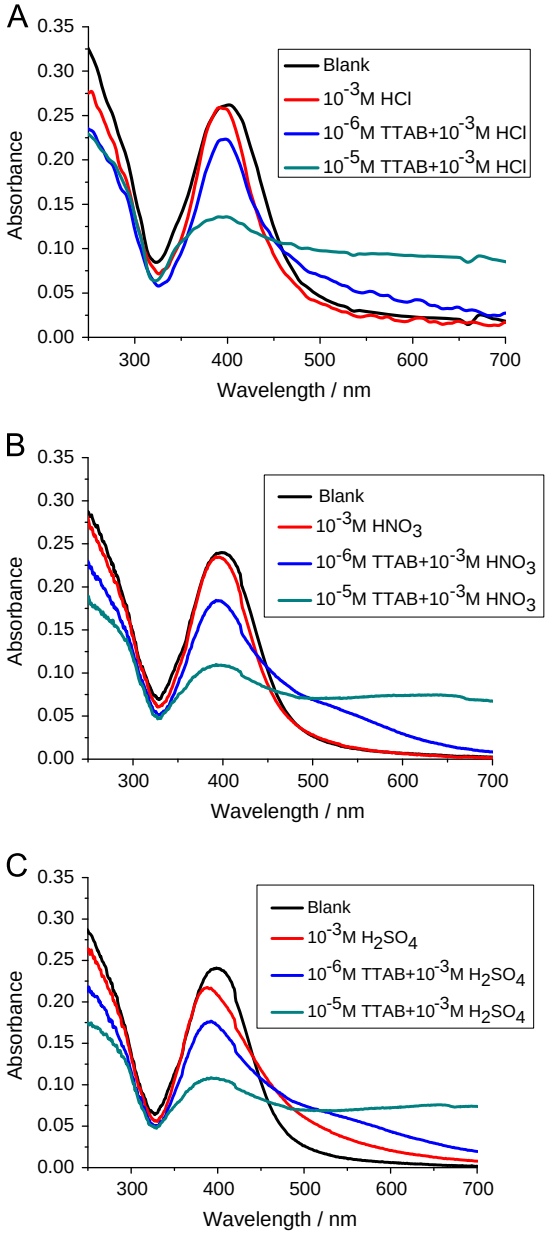

Fig. 5. UV–vis spectra of Ag NPs suspension in the presence of 10^{-3} M different acid with addition of 10^{-6} M and 10^{-5} M TTAB. (A) 10^{-3} M HCl, (B) 10^{-3} M HNO_3, and (C) 10^{-3} M H_2SO_4.

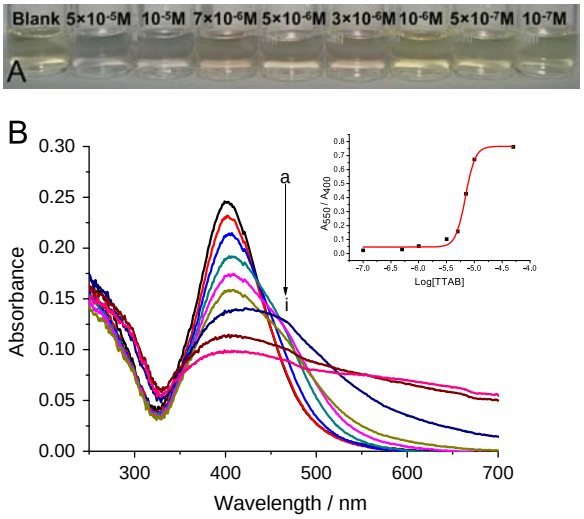

Fig. 6. (A) Colorimetric visualization of TTAB using citrate-capped Ag NPs. TTAB concentrations varied from 10^{-7} M to 5×10^{-5} M. (B) UV–vis spectra of the Ag NPs suspension (pH=3.0 HNO_3) in the presence of different concentrations of TTAB. Inset: plot of A_{550}/A_{400} against log[TTAB]. In the picture, a–i corresponded to the addition of 0, 10^{-7} M, 5×10^{-7} M, 10^{-6} M, 3×10^{-6} M, 5×10^{-6} M, 7×10^{-6} M, 10^{-5} M and 5×10^{-5} M TTAB.

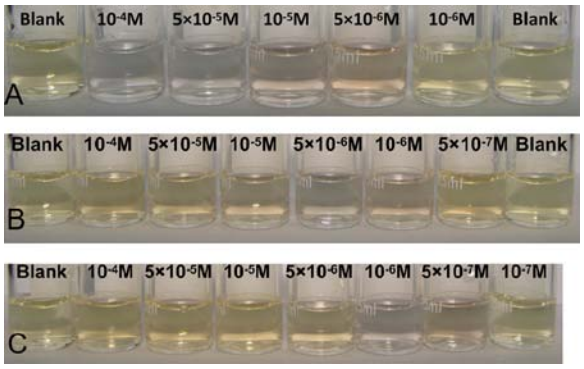

Fig. 7. The visual color change of the Ag NPs solution (pH=3.0 HNO_3) with the addition of a series of concentrations of different quaternary ammonium surfactants. (A) DTAB, (B) CTAB, and (C) STAB.

could be quantified by employing an absorption ratio of A_{550}/A_{400}. A typical plot of this extinction ratio versus TTAB concentration was shown in the inset.

3.3.2. *Cationic surfactants with different lengths of the alkyl chain*

The cationic surfactant had many homologs with different lengths of the alkyl chain. The response of Ag NPs upon the addition of different cationic surfactants including Dodecyl Trimethyl Ammonium Bromide (DTAB), Cetrimonium Bromide (CTAB) and Stearyl Trimethylammonium Bromide (STAB) was investigated and the pictures were shown in Fig. 7. It can be seen that these cationic surfactants responded differently to Ag NPs. The LODs of DTAB, TTAB, CTAB and STAB were 5 μM, 3 μM, 1 μM and 0.5 μM, respectively. The LODs of these surfactants decreased with increase of the length of the carbon chains in surfactant molecules. This should be ascribed to the change of their hydrophobicity. The hydrophobicity of surfactants improved with increase of the length of the carbon chains, and then it was easier to induce the aggregation of Ag NPs. Furthermore, the color of Ag NPs solution changed from yellow to red and then colorless by addition of these four surfactants. However for CTAB and STAB, the color of Ag NPs solution further changed back to yellow from colorless. This could be ascribed to the reversal of the surface charge of Ag NPs with the increasing concentration of CTAB and STAB. When the concentration of cationic surfactants achieved a certain degree, the external anion of citrate-capped Ag NPs was neutralized to saturation, then Ag NPs were modified by cation in turn; thus Ag NPs dispersed again due to the electrostatic repulsion [38,39]. To verify it, the Zeta potential of Ag NPs suspension containing different concentrations of cationic surfactant was evaluated. As is shown in Fig. 8, by increasing the concentration of different cationic surfactants, the Zeta potential values of Ag NPs changed from negative to zero then to positive. The surface of dispersed citrate-capped Ag NPs was negatively charged; thus the Zeta potential of Ag NPs is negative. With the addition of TTAB, the cationic surfactants absorbed onto the surface of Ag NPs and decreased the negative charge of Ag NPs. Meanwhile, Ag NPs began to aggregate. Further with an increase in the concentration of TTAB, the Zeta potential changed to zero and then to positive. This could

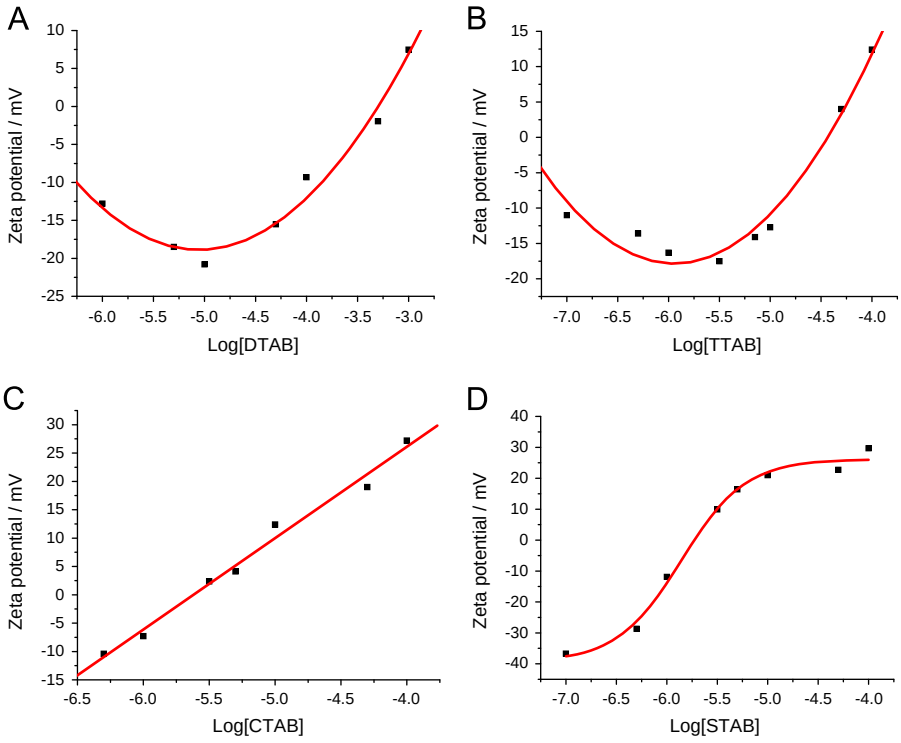

Fig. 8. The plot of Zeta potential against log[concentrations] for the Ag NPs solution (pH=3 HNO_3) with addition of a series of concentrations of different cationic surfactants. (A) DTAB, (B) TTAB, (C) CTAB, and (D) STAB.

well demonstrate the reversal of the surface charge and redispersion of Ag NPs.

What is more, Fig. 9 shows the plots of A_{550}/A_{400} against log [concentrations] for the Ag NPs solution (pH=3 HNO_3) with the addition of a series of concentrations of different cationic surfactants. For CTAB and STAB, the plots increased to maximum and then decreased, which indicated the aggregation and deaggregation of Ag NPs. Also the aggregation of Ag NPs by CTAB and STAB occurred at much lower concentration than by DTAB and TTAB.

3.3.3. *Benzalkonium Bromide (BZKB)*

BZKB is a cationic surfactant with dodecyl group which is the same as DTAB. BZKB could be obtained by displacing one methyl group of DTAB by benzyl group. Compared to DTAB, the hydrophobicity of BZKB is stronger. The response of Ag NPs solution to BZKB is more sensitive. As can be seen in Fig. 10, the LOD of BZKB is 3 μM which is lower than that of DTAB.

3.4. *Selectivity*

According to the aggregation mechanism of the citrate-capped Ag NPs, anion and neutral surfactants could not induce its aggregation, which was identified with the experimental results (Fig. 11).

3.5. *Real sample analysis*

In the real sample assays, the disinfectant residual sample containing BZKB was added into Ag NPs suspension with different dilution multiples. As shown in Fig. 12, a clear color change from yellow to red then to colorless and finally to yellow again was observed. According to this color change of Ag NPs solution, the concentration of BZKB is about 6×10^{-4} M in the disinfectant residual sample. This indicated that it could be used as a semi-quantitative analysis method for BZKB detection.

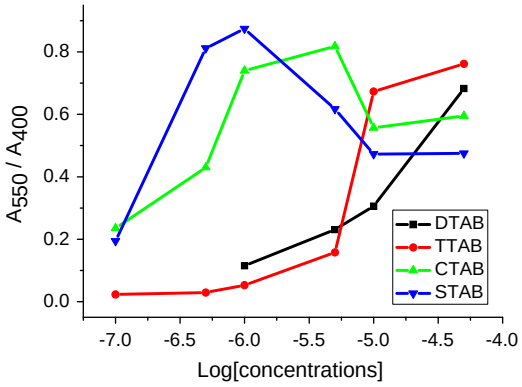

Fig. 9. Plots of A_{550}/A_{400} against log[concentrations] for the Ag NPs solution (pH=3 HNO_3) with addition of a series of concentrations of different cationic surfactants.

Fig. 10. Colorimetric visualization of BZKB using citrate-capped Ag NPs. BZKB concentrations varied from 10^{-6} M to 10^{-3} M.

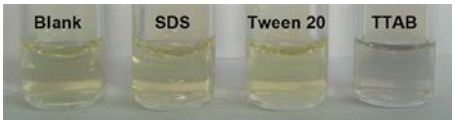

Fig. 11. Colorimetric response of Ag NPs solution (pH=3 HNO_3) upon the addition of 10 μM various surfactants.

4. Conclusions

In this paper, a low-cost, sensitive, simple and rapid colorimetric method using citrate-capped Ag NPs to detect cationic surfactants

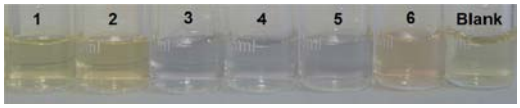

Fig. 12. Colorimetric response of the Ag NPs (pH = 3.0 HNO_3) upon the addition of different dilution multiple of the disinfectant residual sample containing BZKB. In the picture, 1–6 corresponded to the sample dilution multiple of 2, 4, 20, 40, 66 and 200 times.

was developed. It is the first time that hydrophobic effect of cationic surfactant to induce the aggregation of Ag NPs is reported. The LODs of different cationic surfactants were in the range of 0.5–5 μM. These advantages are likely to provide a promising application for the simple, on-site detection of cationic surfactants. This detection method was successfully utilized to the disinfectant residual sample.

Acknowledgments

This work was supported by the National Instrumentation Program of China (2011YQ17006711), the Major Program of NSFC (21190044), the NSFC Scientific Equipment Joint Fund Project (11179004) and NSFC Innovative Research Group Project (21121091).

Appendix A. Supplementary material

Supplementary data associated with this article can be found in the online version at http://dx.doi.org/10.1016/j.talanta.2013.10.009.

References

[1] M.G. Murphy, M. Al-Khalidi, J.F.S. Crocker, Chemosphere 59 (2005) 235.
[2] Hsueh-Ying Liu, Wang-Hsien Ding, J. Chromatogr. A 1025 (2004) 303.
[3] Mudunic-Cacic, D. Sak-Bosnar, M. GalovicO., Talanta 76 (2008) 259.
[4] Andjelija Malenovic, Darko Ivanovic, Biljana Jancic, Acta Chim. Slov. 51 (2004) 559.
[5] A. Malenovic, M. Medenica, D. Ivanovic, Farmaco 60 (2005) 157.
[6] A.R. Hind, S.K. Bhargava, S.C. Grocott, J. Chromatogr. A 765 (1997) 287.
[7] W.H. Ding, P.C. Tsai, Anal. Chem. 75 (2003) 1792.
[8] C. Li, M. Numata, M. Takeuchi, Angew. Chem. Int. Ed. 44 (2005) 6371.
[9] Aihui Liang, QingyeLiu, Zhiliang Jiang, TrendsAnal. Chem. 37 (2012) 32.
[10] Hong Ying Zhou, Chang Zhao, Li, Yujian Heet al., Talanta 97 (2012) 331.
[11] H. Nakashima, N. Yoshida, Chem. Lett. 35 (2006) 1168.
[12] J. Qian, X. Qian, Y. Xu, Chem.–Eur. J. 15 (2009) 319.
[13] Hua Deng, XuZhang, Xiaoning Zhang, Chem. Commun. 49 (2013) 51.
[14] Zitong Yizhen Liu, Wu, Jiming Hu, Chem. Commun. 48 (2012) 3164.
[15] Hui Wei, Bingling Li, Shaojun Dong, Chem. Commun. (2007) 3735.
[16] J.-S. Lee, P.A. Ulmann, M.S. Han, Nano Lett. 8 (2008) 529.
[17] Mohammed I. Shukoor, Meghan O. Altman, Weihong Tan, ACS Appl. Mater. Interfaces 4 (2012) 3007.
[18] Chia-Chen Chang, Shih-ChungWei, Chii-Wann Lin, Biosensors Bioelectronics 42 (2013) 119.
[19] J. Liu, Y. Lu, ALihua Wang, Chunhai Fan, Small 4 (2008) 1196.
[20] Huan Jiang, Zhaohui Chen, Haiyan Cao, Yuming Huang, Analyst 137 (2012) 5560.
[21] Zhong De Liu, Hai Yan Zhu, Heng Xin Zhao, Cheng Zhi Huang, Talanta 106 (2013) 255.
[22] S. Kim, J.W. Park, D. Kim, Angew. Chem. Int. Ed. 48 (2009) 4138.
[23] Ying Xue, Hong Zhao, Zhijiao Wu, Xiangjun Li, YujianHe, Zhuobin Yuan, Analyst 136 (2011) 3725.
[24] Yuangen Wu, Shenshan Zhan, Pei Zhou, Chem. Commun. 48 (2012) 4459.
[25] J.S. Lee, A.K.R. Lytton-Jean, S.J. Hurst, Nano Lett. 7 (2007) 2112.
[26] Cuie Youhui Lin, Chen, Jinsong Ren, Chem. Commun. 47 (2011) 1181.
[27] Yu-rong Ma, Hong-yun Niu, Ya-qi Cai, Chem. Commun. 47 (2011) 12643.
[28] Shan Chen, Yi-Min Fang, Jian-Jun Sun, Analyst 137 (2012) 2021.
[29] Siqiu Ye, Xinhao Shi, Wei Gu, YixuanZhang, Yuezhong Xian, Analyst 137 (2012) 3365.
[30] Guangke He, Liang Zhao, Kai Chen, Yuanyuan Liu, Hongjun Zhu, Talanta 106 (2013) 73.
[31] Cuiping Han, Haibing Li, Analyst 135 (2010) 583.
[32] Eugenii Katz, Itamar Willner, Angew. Chem. Int. Ed. 43 (2004) 6042.
[33] N.L. Rosi, C.A. Mirkin, Chem. Rev. 105 (2005) 1547.
[34] James E. Ghadiali, Molly M. Stevens, Adv. Mater. 20 (2008) 4359.
[35] Hui Wei, Chaogui Chen, Bingyan Han, Erkang Wang, Anal. Chem. 80 (2008) 7051.
[36] Y. Kim, R.C. Johnson, J.T. Hupp, Nano Lett. 1 (2001) 165–167.
[37] Juan Li, Hua-E. Fu, Ling-Jie Wu, Ai-Xian Zheng, Guo-Nan Chen, Huang-Hao Yang, Anal. Chem. 84 (2012) 5309–5315.
[38] Marilyn X. Zhou, Joe P. Foley, Anal. Chem. 78 (2006) 1849–1858.
[39] Edit Csapó, Rita Patakfalvi, Viktória Hornok, László Tamás Tóth, Áron Sipos, Anikó Szalai, Mária Csete, Imre Dékány, Colloids Surf. B: Biointerfaces 98 (2012) 43–49.